iScience

CellPress
OPEN ACCESS

Article

Pro- and anti-apoptotic fate decisions induced by di- and trimeric synthetic cytokine receptors

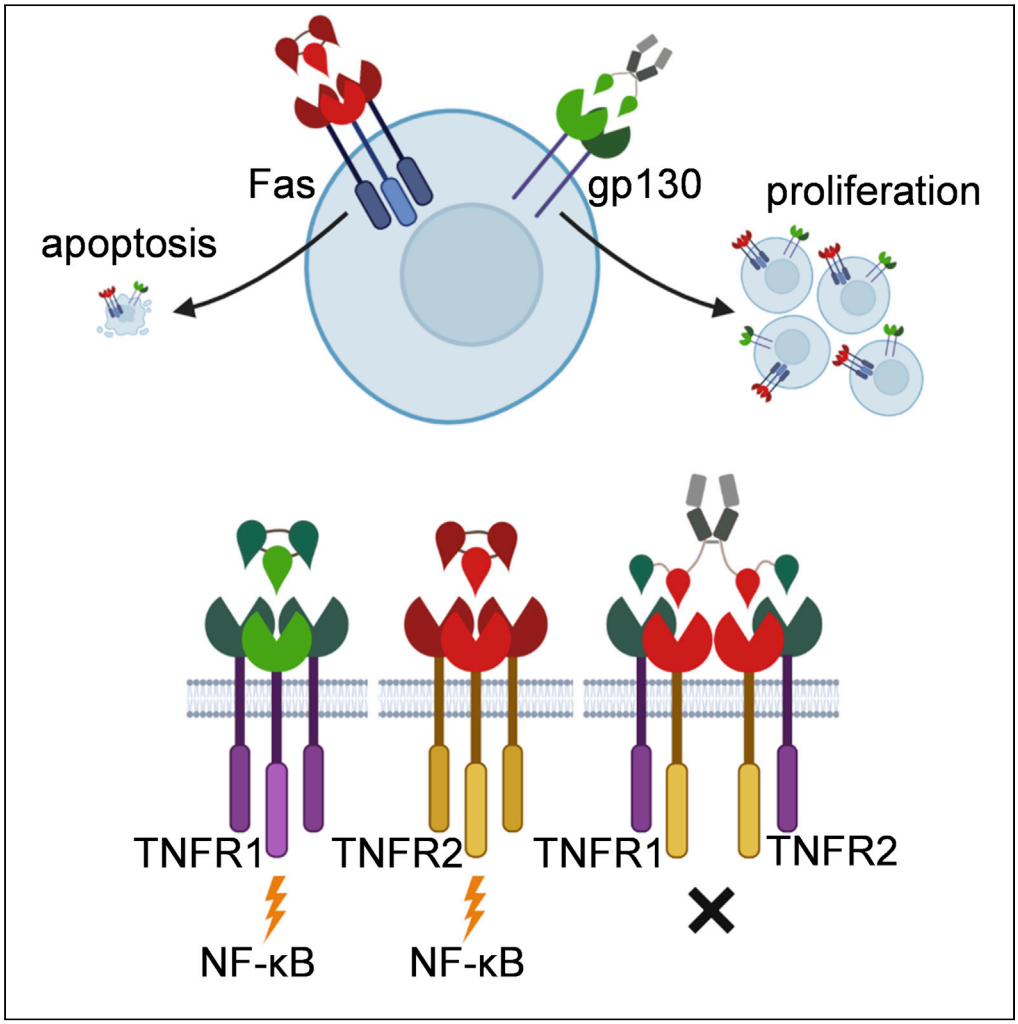

Sofie Mossner, Doreen Manuela Floss, Jürgen Scheller

jscheller@uni-duesseldorf.de

Highlights

SyCyRs induce TNFR1 or TNFR2 mediated NF-κB activation as trimers or oligomers.

Fas-SyCyR induces Caspase-induced apoptosis as trimer and as dimer.

Synthetic loss of function Fas-SyCyR fails to induce Caspase mediated apoptosis.

gp130-and Fas-SyCyR in one cell enable proliferation via gp130 or apoptosis via Fas.

Mossner et al., iScience 24, 102471
May 21, 2021
https://doi.org/10.1016/j.isci.2021.102471

iScience

CellPress
OPEN ACCESS

Article

Pro- and anti-apoptotic fate decisions induced by di- and trimeric synthetic cytokine receptors

Sofie Mossner,[1] Doreen Manuela Floss,[1] and Jürgen Scheller[1,2,*]

SUMMARY

Synthetic strategies to activate cytokine receptors so far only address standard dimeric cytokine receptor assemblies. The 19 ligands of the tumor necrosis factor superfamily (TNFSF), however, form noncovalent trimers and receptor trimerization is considered to be essential for receptor activation. Synthetic TNFR1, TNFR2, and Fas/CD95 receptors were activated by synthetic trimeric ligands which induced NF-κB signaling or Caspase-induced apoptosis. Albeit dimeric receptor activation did not induce synthetic TNFR1 and TNFR2 signaling, dimeric FasL induced extenuated apoptosis. Simultaneous integration of dimeric Interleukin (IL-)6 receptor gp130 and trimeric Fas as synthetic cytokine receptors in one cell enabled binary cell fate decisions, gp130-mediated proliferation or Fas-mediated apoptosis. In summary, our modular fully synthetic cytokine signaling system allows precisely orchestrated cellular responses to selectively induce pro- and anti-apoptotic signaling via canonical dimeric receptors of the IL-6 family and non-canonical trimeric receptor complexes of the TNF superfamily.

INTRODUCTION

Immunoregulatory cytokines such as Interleukin (IL-)6, TNF, and FasL are critically involved in a plethora of physiological and pathophysiological processes including autoimmunity and cancer development (Scheller et al., 2019). Typically, cytokines induce transmembrane receptor dimerization and switch them from the off-state to the on-state. An emerging field to analyze these processes and for the development of personalized therapies is synthetic biology (Chakravarti and Wong, 2015). One breakthrough was the approval of the first gene therapy: chimeric antigen receptor (CAR) T cell immunotherapy for acute lymphoblastic leukemia (ALL) (Si et al., 2018). Currently, many researchers are working on various synthetic approaches for the improvement of the system to increase its safety and to make it applicable for more diseases (Caliendo et al., 2019). Recently, we have designed a new dimeric synthetic cytokine receptor (SyCyRs) system to phenocopy IL-6/IL-23 and IL-22 signaling (Engelowski et al., 2018; Mossner et al., 2020a). SyCyRs use nanobodies as extracellular ligand binding domain (Fridy et al., 2014; Rothbauer et al., 2008), fused to the transmembrane and intracellular domain of the receptor of interest (Wesolowski et al., 2009). Nanobodies serve as sensors for homo- or heterodimeric ligands, e.g., GFP/mCherry fusion proteins (Mossner et al., 2020b). Binding of the synthetic ligand to its synthetic receptor then activates the SyCyRs and the endogenous signaling pathway of the intracellular receptor of interest is specifically activated without any background activation (Engelowski et al., 2018; Mossner et al., 2020a). We hypothesized that this modular ligand assembly should also allow homo-/heterotrimeric receptor assemblies (Engelowski et al., 2018; Mossner et al., 2020a, 2020b). The tumor necrosis factor superfamily (TNFSF) consists of 19 ligands and 29 related receptors (Dostert et al., 2019; Vanamee and Faustman, 2018b). TNFSF receptors (TNFRSF) can be classified into death and non-death receptors (Aggarwal, 2003; Dostert et al., 2019; Locksley et al., 2001). Death receptors possess a conserved death domain of 80 amino acids for caspase activation (Arul M. Chinnaiyan et al., 1995) while non-death receptors interact with TNFR-associated factors (TRAFs) (P.W. Dempsey et al., 2003) to initiate survival mainly by NF-κB (Shishodia and BB, 2004). Here, we focused on the trimeric death receptors TNFR1, Fas, TrailR1, and TrailR2 as well as the TRAF-interacting receptor TNFR2. TNFR1 and TNFR2 are both activated by TNFα, all of which are present as preformed trimers (Bodmer et al., 2002; Locksley et al., 2001; Cabal-Hierro and Lazo, 2012). Binding of TNFα to the TNFR1 eventually leads to caspase or NF-κB activation (Faustman and Davis, 2010; Brenner et al., 2015), whereas trimeric activation of Fas, TrailR1/2 complexes selectively induces caspase-mediated apoptosis (David R. McIlwain et al., 2015; E. M. Creagh and Martin, 2001). Recent data suggests also higher-than-trimeric receptor oligomerization upon activation (Vanamee and

[1]Institute of Biochemistry and Molecular Biology II, Medical Faculty, Heinrich-Heine-University, 40225 Düsseldorf, Germany

[2]Lead contact

*Correspondence: jscheller@uni-duesseldorf.de

https://doi.org/10.1016/j.isci.2021.102471

Faustman, 2020), comparable to cluster-activation seen for T-cell receptors (Grakoui et al., 1999). Targeted analysis of TNFRSF members is also of importance, because mutations in TNFSF/TNFRSF members can lead to various diseases among them, such as TNF receptor-associated periodic syndrome (TRAPS) (Savic et al., 2012) or autoimmune lymphoproliferative syndrome (ALPS) (Anke M.J. Peters et al., 1999).

Current strategies in SyCyRs signaling did not, however, address trimeric receptor assemblies. Therefore, we generated SyCyRs for trimeric cytokine receptors of the TNFRSF family.

RESULTS

Trimeric assembly of synthetic cytokine receptors for TNFR1 and 2 induces NFκB activation

We hypothesized that our synthetic cytokine receptor system based on multimerized units in which each unit engages a single receptor should also allow assembly of the higher-than-dimeric receptor complexes found in the tumor necrosis factor receptor superfamily (TNFRSF). First, the GFP- (G_{VHH}) and mCherry-nanobodies (C_{VHH}) were genetically fused to the transmembrane and intracellular domains of TNFR1 and TNFR2 (Figures 1A and S1A). Synthetic receptors were introduced into the murine pre-B cell line Ba/F3 which also express the Interleukin (IL)-6 receptor chain gp130 and therefore proliferate in the presence of Hyper-IL-6, which is a fusion protein of IL-6 and the soluble IL-6R in a process called trans-signaling (Schmitz et al., 2000). Cell surface expression of G_{VHH}TNFR1, C_{VHH}TNFR1, and C_{VHH}TNFR2 was verified by flow cytometry (Figure S1B). Recently, we described Fc-tagged GFP and mCherry fusion proteins as alternative synthetic cytokine ligands, which exhibit increased stability and enable efficient protein purification via Protein A affinity chromatography (Mossner et al., 2020b) (Figure S2A). In order to assemble receptors in higher-than-dimeric oligomers, trimeric GFP_3 and $mCherry_3$ (Mossner et al., 2020b), and hexameric Fc-tagged fusion proteins of 3xGFP (3xGFP-Fc) or 3xmCherry (3xmCherry-Fc) were generated (Figures S2A and S2B). CHO-K1 cells were stably transduced with cDNAs coding for 3xGFP-Fc or 3xmCherry-Fc fusion proteins. Fc-fusion proteins were purified from clonal CHO-K1 cell culture supernatants by Protein A-Sepharose chromatography (Figures S3A and S3B). The overall yield was 433 μg 3xGFP-Fc/L and 363 μg 3xmCherry-Fc/L. The Fc-mediated formation of hexameric synthetic ligands was demonstrated by SDS-Page followed by Western blotting under reducing and non-reducing conditions (Figures S3C and S3D). Moreover, GFP-mCherry was purified via Twin-Strep-tag from CHO-K1 cells with an overall yield of 4.6 mg/L to activate heterodimeric synthetic cytokine receptors (Figures S3E and S3F). Ba/F3 cells expressing synthetic TNF receptor variants were stimulated with these GFP- and mCherry-fusion proteins and phosphorylation of IκB (pIκB) as indicator of NF-κB activation was determined by Western blotting. For Ba/F3/gp130/G_{VHH}TNFR1/C_{VHH}TNFR1 cells trimeric GFP_3 and hexameric 3xGFP-Fc induced phosphorylation of IκB via the G_{VHH}TNFR1 receptor while trimeric $mCherry_3$ and hexameric 3xmCherry-Fc induced phosphorylation of IκB via the C_{VHH}TNFR1 SycyR (Figure 1B). Tetrameric GFP-mCherry-Fc was also able to induce phosphorylation of IκB by activating the receptors as tetramer with 2xG_{VHH}TNFR1 and 2xC_{VHH}TNFR1 receptor chains. Coevally, dimeric GFP-Fc and mCherry-Fc failed to induce pIκB (Figure 1B). Further, Ba/F3/gp130/G_{VHH}TNFR1/C_{VHH}TNFR2 cells were also stimulated with GFP and mCherry fusion proteins. Again, trimeric GFP_3 and hexameric 3xGFP-Fc induced G_{VHH}TNFR1-mediated pIκB, whereas for this cell line trimeric $mCherry_3$ and hexameric 3xmCherry-Fc induced C_{VHH}TNFR2-mediated pIκB. Stimulation of the cells with GFP-mCherry-Fc now mediated a heterotetramer consisting of 2xG_{VHH}TNFR1 and 2xC_{VHH}TNFR2, which however did not result in the phosphorylation of IκB (Figure 1C).

Next, Ba/F3/gp130/G_{VHH}TNFR1/C_{VHH}TNFR2 cells were stimulated with increasing concentrations of GFP_3 or $mCherry_3$. Phosphorylation of pIκB was maximal for about 100 ng/mL GFP_3 and $mCherry_3$ (Figure 1D). Consequently, GFP_3 and $mCherry_3$-induced pIκB via G_{VHH}TNFR1 and C_{VHH}TNFR2 was efficiently inhibited via the IKK inhibitor IKK-2 (Figure 1E) (Lin et al., 2010). Ba/F3/gp130 cells proliferate following STAT3 and ERK activation, however, NFκB-activation by G_{VHH}TNFR1 and C_{VHH}TNFR2 was not sufficient to induce cellular proliferation (Figure S3G). Expression of exemplified NF-κB target genes FasL, Traf1, IL-6 and TNFα by quantitative RT-PCR showed a significant increase in the gene expression of IL-6 and TNFα by G_{VHH}TNFR1 and of FasL and Traf1 for the activation of both G_{VHH}TNFR1 and C_{VHH}TNFR2 (Figure 1F). Our data demonstrated for the first time that trimeric synthetic cytokine ligands were able to activate synthetic trimeric receptor complexes. Taken together, we showed that trimeric and higher ordered GFP and mCherry fusion proteins activated synthetic homotrimeric G_{VHH}TNFR1 and C_{VHH}TNFR2 complexes, whereas mixed receptor complexes were not biologically active. Since the TNFRSF also harbors death receptors, the next step was to analyze if the SyCyRs system can also be applied here given that until now the SyCyRs were only utilized with anti-apoptotic receptors like IL-6R, gp130 or IL-10Rβ (Engelowski et al., 2018; Mossner et al., 2020a).

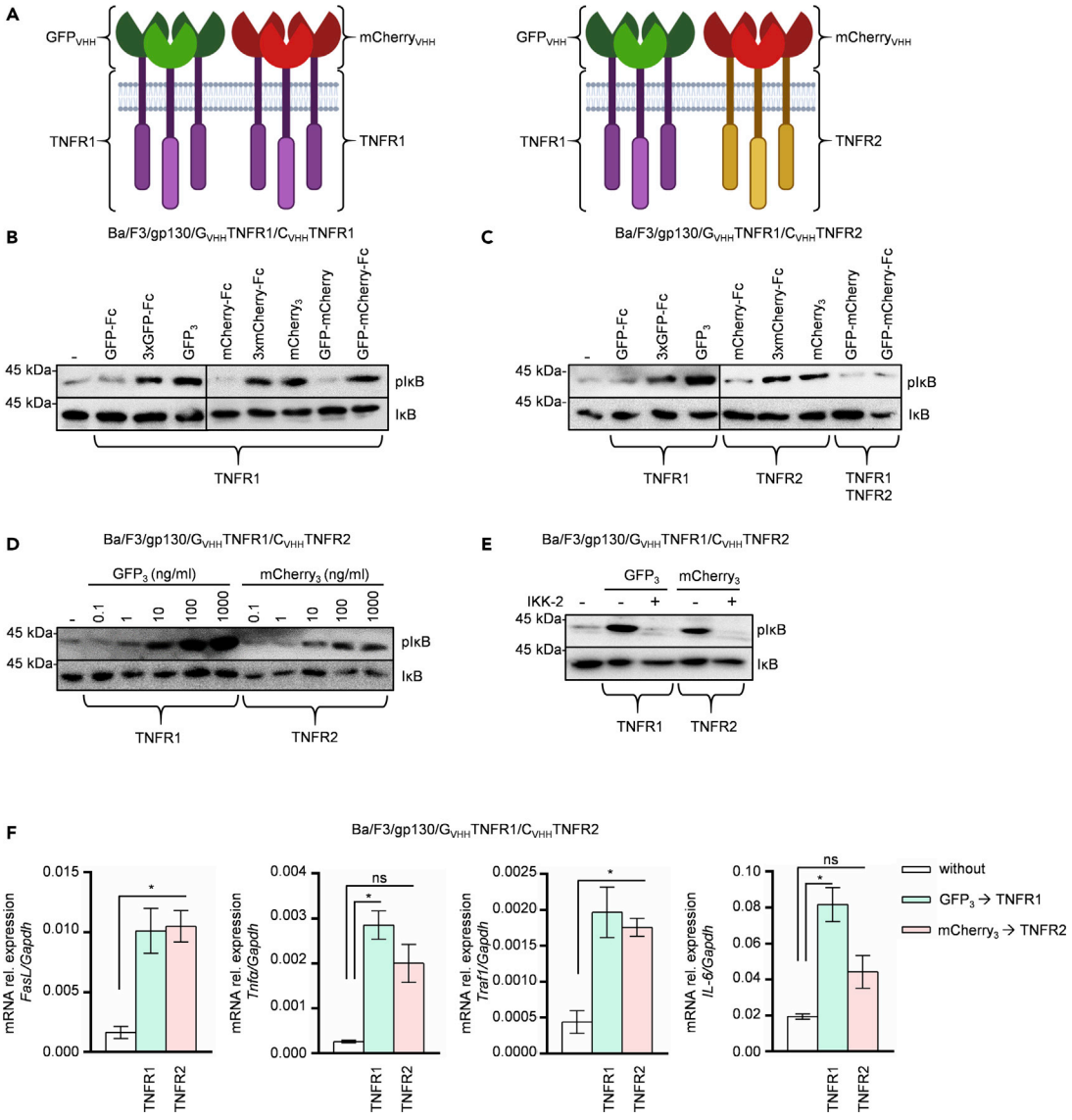

Figure 1. Phenocopy of TNFR1 and TNFR2 signaling via NF-κB signal pathway using synthetic G$_{VHH}$TNFR1, C$_{VHH}$TNFR1 and C$_{VHH}$TNFR2 cytokine receptors

(A) Schematic illustration of one cell line expressing GFP$_{VHH}$TNFR1 (green, violet) and mCherry$_{VHH}$TNFR1 (red, violet) and one cell line expressing GFP$_{VHH}$TNFR1 (green, violet) and mCherry$_{VHH}$TNFR2 (red, violet). Created with BioRender.com.

(B) Phosphorylation of IκB in Ba/F3/gp130/G$_{VHH}$TNFR1/C$_{VHH}$TNFR1 cells treated without cytokine or with 100 ng/mL GFP-Fc, 3xGFP-Fc, GFP$_3$, mCherry-Fc, 3xmCherry-Fc, mCherry$_3$, GFP-mCherry, GFP-mCherry-Fc for 60 min. Before stimulation cells were pre-incubated with 2.5 μM MG132 for 30 min. Equal amounts of protein (50 μg/lane) were analyzed via specific antibodies detecting phospho-IκB or IκB.

(C) Phosphorylation of IκB in Ba/F3/gp130/G$_{VHH}$TNFR1/C$_{VHH}$TNFR2 cells treated without cytokine or with 100 ng/mL GFP-Fc, 3xGFP-Fc, GFP$_3$, mCherry-Fc, 3xmCherry-Fc, mCherry$_3$, GFP-mCherry, GFP-mCherry-Fc for 60 min. Before stimulation cells were pre-incubated with 2.5 μM MG132 for 30 min. Equal amounts of protein (50 μg/lane) were analyzed via specific antibodies detecting phospho-IκB or IκB.

(D) Ba/F3/gp130/G$_{VHH}$TNFR1/C$_{VHH}$TNFR2 cells were stimulated without cytokine or with increasing concentrations from 0.1–1000 ng/mL of GFP$_3$ or mCherry$_3$ for 60 min. Cells were incubated with 2.5 μM MG132 for 30 min prior to stimulation. Equal amounts of protein (50 μg/lane) were analyzed via specific antibodies detecting phospho-IκB or IκB.

(E) Ba/F3/gp130/G$_{VHH}$TNFR1/C$_{VHH}$TNFR2 cells were treated without cytokine or with 100 ng/mL GFP$_3$ or mCherry$_3$ for 60 min. Before stimulation cells were pre-incubated with 2.5 μM MG132 for 30 min. Cells treated with 100 ng/mL GFP$_3$ or mCherry$_3$ and IKK-2 inhibitor were stimulated for 60 min and pre-incubated with the 18 μM IKK-2 for 30 min. Equal amounts of protein (50 μg/lane) were analyzed via specific antibodies detecting phospho-IκB and IκB.

(F) Quantification of NF-κB target genes *FasL*, *Traf1*, *IL-6* and *Tnfα* in Ba/F3/gp130/G$_{VHH}$TNFR1/C$_{VHH}$TNFR2 cells stimulated without cytokine or with 100 ng/mL GFP$_3$ (TNFR1) or mCherry$_3$ (TNFR2) for 60 min. Error bars indicate S.D., p value was determined using one-way ANOVA *, $p < 0.05$.(B-F) One representative experiment out of three is shown.

Trimeric assembly of synthetic cytokine receptors for death receptors induces apoptosis

Naturally, death ligands such as FasL ligand (FasL) and Trail signal also via homotrimeric death receptors Fas or TrailR resulting in induction of extrinsic apoptosis via Caspase activation (Wilson et al., 2009). Here, we selected the prototypic death receptor Fas/CD95 and the two Trail receptors TrailR1 and TrailR2 for reformatting into synthetic death receptors (Figures 2A and S4A). All synthetic cytokine receptors were introduced into Ba/F3/gp130 and cell surface expression of G_{VHH}Fas and C_{VHH}Fas, C_{VHH}TrailR1, and C_{VHH}TrailR2 was shown by flow cytometry (Figure S4B). Ba/F3/gp130 cells expressing C_{VHH}TrailR1, C_{VHH}TrailR2, C_{VHH}Fas or G_{VHH}Fas were analyzed for inhibition of Hyper-IL-6-induced cellular proliferation by stimulation with hexameric mCherry- or GFP-Fc-fusion proteins. Co-incubation of Hyper-IL-6 and 3xmCherry-Fc did not significantly inhibit cellular proliferation of C_{VHH}TrailR1 and C_{VHH}TrailR2-expressing cells compared to Hyper-IL-6 stimulated cells (Figure 2B), whereas C_{VHH}Fas and G_{VHH}Fas-expressing cells, incubated with 3xmCherry-Fc or 3xGFP-Fc, completely failed to proliferate, suggesting that the synthetic Fas induced apoptosis. Therefore, we decided to focus on synthetic Fas in further experiments. Interestingly, also dimeric GFP-Fc and mCherry-Fc inhibited Hyper-IL-6 induced proliferation of Ba/F3/gp130/G_{VHH}Fas and Ba/F3/gp130/C_{VHH}Fas cells, respectively (Figures 2C and S5A), albeit Fas was considered to be specifically activated by trimerization (Jason R. Orlinick et al., 1997; Starling et al., 1997).

Next, we introduced the loss-of-function death domain mutation E256G (Anke M.J. Peters et al., 1999) into C_{VHH}Fas (Figures 2D,S5B, and S5C) and Hyper-IL-6 induced proliferation of Ba/F3/gp130/$C_{VHH}Fas_{E256G}$ cells was not inhibited by co-stimulation with mCherry-Fc or 3xmCherry-Fc (Figure 2E). IC_{50} values of synthetic FasL ligands were determined to be 2.96 ng/mL (261 pM) for 3xGFP-Fc, 0.23 ng/mL (26.9 pM) for GFP_3 and 5.47 ng/mL (935 pM) for GFP-Fc in Ba/F3/gp130/G_{VHH}Fas and 0.98 ng/mL (89.3 pM) for 3xmCherry-Fc, 0.14 ng/mL for $Cherry_3$ (17 pM) and 0.50 ng/mL (87.4 pM) for mCherry-Fc in Ba/F3/gp130/C_{VHH}Fas cells (Figures 3A and S6A). These data showed that low ng/ml amounts were sufficient to efficiently prevent Hyper-IL-6 induced proliferation of Ba/F3/gp130 cells expressing synthetic Fas variants. Furthermore, it seems that the trimeric ligands GFP_3 and $mCherry_3$ induce apoptosis more efficiently than the hexameric ligands because they have a lower IC_{50} concentration. Ba/F3/gp130/$C_{VHH}Fas_{E256G}$ cells were also incubated with up to 1 µg/mL 3xmCherry-Fc but also a high concentration of the ligand was not able to impair Hyper-IL-6 induced proliferation (Figure S6B).

A hallmark of apoptosis is the activation of Caspase 3 which can be visualized by Western blotting as loss of full-length pro-Caspase 3 (Porter and RU, 1999). To assess the ability of synthetic FasL ligands to induce apoptosis, Ba/F3/gp130/G_{VHH}Fas and Ba/F3/gp130/C_{VHH}Fas cells were stimulated with Hyper-IL-6 and synthetic ligands. As depicted in Figures 3B and S6C, Hyper-IL-6 induced sustained STAT3 phosphorylation (pSTAT3) in Ba/F3/gp130/G_{VHH}Fas and Ba/F3/gp130/C_{VHH}Fas cells. Stimulation with GFP_3 and 3xGFP-Fc or $mCherry_3$ and 3xmCherry-Fc but not monomeric or dimeric mCherry and GFP induced cleavage of pro-Caspase 3 after 6 hr. Here, we can conclude again that the activation of apoptosis by the trimeric ligands is faster than for the hexameric or dimeric ligands. Importantly, decreased pSTAT3 was detected at the time of Caspase 3 activation indicating advanced apoptotic progression. No cleaved Caspase 3 was detected if the cells were co-incubated with the Caspase 3 inhibitor QVD (Figure 3C). Additionally, a time dependent increase in cleaved Caspase 3 was detected between 2 and 4 hr activation of the Fas-SyCyR (Figure 3C). Stimulation of Ba/F3/gp130 cells expressing $C_{VHH}Fas_{E256G}$ with mCherry-Fc and 3xmCherry-Fc did not, however, result in Caspase 3 activation and downregulation pSTAT3 (Figure 3D).

To further analyze apoptosis progression, we performed flow cytometry staining of 7-AAD and Annexin V of Ba/F3/gp130 cells expressing G_{VHH}Fas or C_{VHH}Fas stimulated for 24 and 48 hr with Hyper-IL-6 and synthetic ligands. Importantly, with Hyper-IL-6 93.7% of the Ba/F3/gp130/G_{VHH}Fas cells and 84.7% of the Ba/F3/gp130/C_{VHH}Fas cells were alive, whereas incubation with 70% EtOH resulted in 99.0% and 98.9% of dead cells (Tables 1 and 2, Figures S7A andS7B). Co-stimulation of Hyper-IL-6 and monomeric GFP or mCherry did not increase the amount of late apoptotic cells, whereas 3xGFP-Fc, GFP_3 or 3xmCherry-Fc, $mCherry_3$ resulted in 92.3%, 94.0% or 62.2%, 70.1% late apoptotic cells, respectively. Again, after 24 hr of co-stimulation also dimeric GFP-Fc and mCherry-Fc led to a significant but lower increase of the late apoptotic cell population to 31.7% and 18.0% (Tables 1 and 2, Figures S7A andS7B). The cells were also incubated for 48 hr and interestingly, co-incubation of Hyper-IL-6 with dimeric GFP-Fc or mCherry-Fc showed an increasing number of apoptotic cells at later time points. After 48 hr 63.9% of Ba/F3/gp130/G_{VHH}Fas cells were in late apoptosis. For Ba/F3/gp130/C_{VHH}Fas cells 40.5% were in late apoptosis after 48 hr. Ba/F3/gp130/G_{VHH}Fas or Ba/F3/gp130/C_{VHH}Fas cells incubated with Hyper-IL-6 and 3xGFP-Fc, GFP_3 or 3xmCherry-Fc, $mCherry_3$ showed that after 48 hr already 95.4% (3xGFP-Fc),

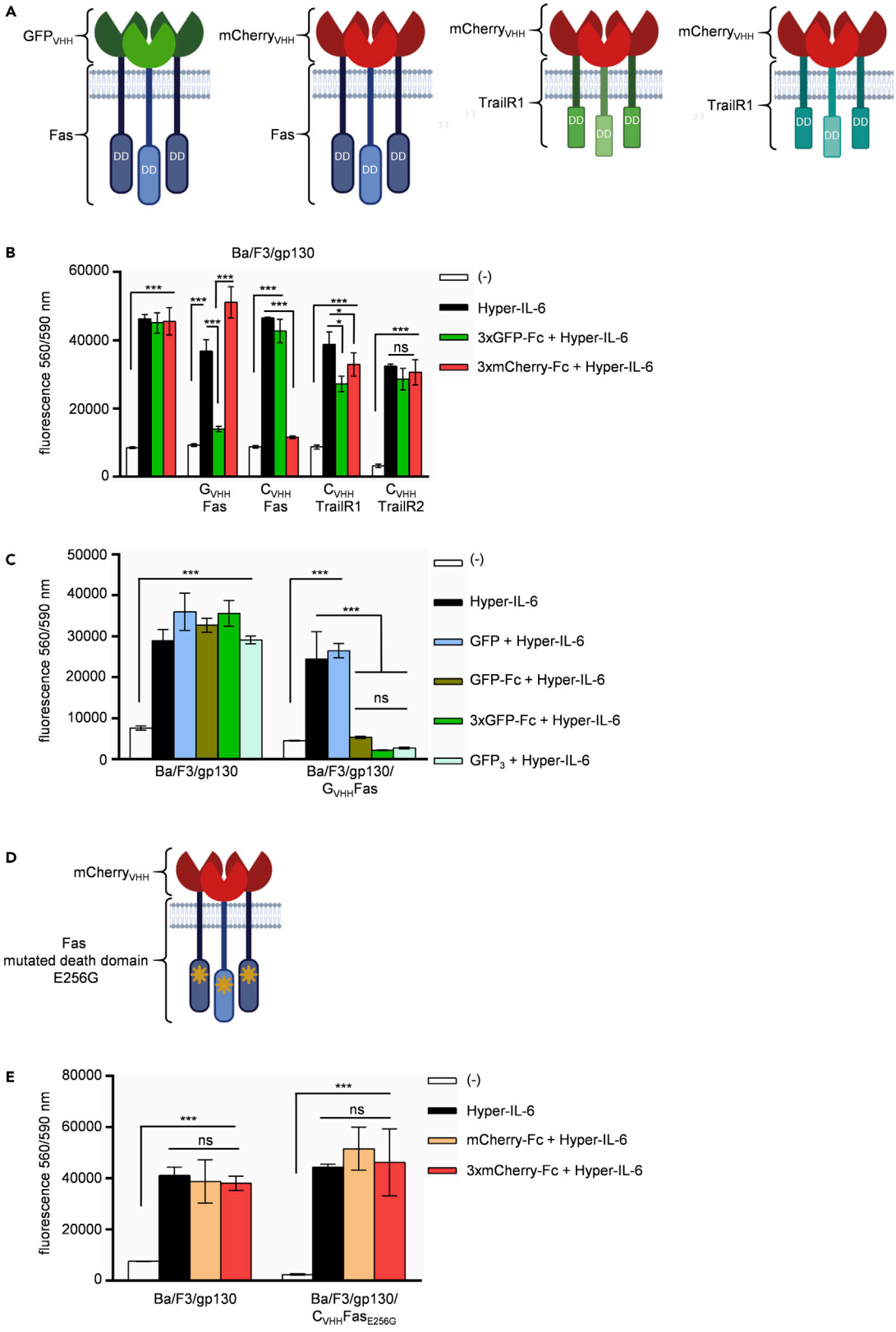
A
GFP$_{VHH}$
Fas
DD
mCherry$_{VHH}$
TrailR1
B
Ba/F3/gp130
fluorescence 560/590 nm
(-)
Hyper-IL-6
3xGFP-Fc + Hyper-IL-6
3xmCherry-Fc + Hyper-IL-6
G$_{VHH}$ Fas
C$_{VHH}$ Fas
C$_{VHH}$ TrailR1
C$_{VHH}$ TrailR2
C
GFP + Hyper-IL-6
GFP-Fc + Hyper-IL-6
3xGFP-Fc + Hyper-IL-6
GFP$_3$ + Hyper-IL-6
Ba/F3/gp130/ G$_{VHH}$Fas
D
Fas mutated death domain E256G
E
mCherry-Fc + Hyper-IL-6
3xmCherry-Fc + Hyper-IL-6
Ba/F3/gp130/ C$_{VHH}$Fas$_{E256G}$

Figure 2. Synthetic cell death receptors Fas, TrailR1 and TrailR2

(A) Schematic illustration of cell lines expressing either GFP_{VHH}Fas (green, blue), $mCherry_{VHH}$Fas (red, blue), $mCherry_{VHH}$TrailR1 (red, green) or $mCherry_{VHH}$TrailR2 (red, turquois). Created with BioRender.com.

(B) Proliferation of Ba/F3/gp130, Ba/F3/gp130/G_{VHH}Fas, Ba/F3/gp130/C_{VHH}Fas, Ba/F3/gp130/C_{VHH}TrailR1 and Ba/F3/gp130/C_{VHH}TrailR2 cells incubated without cytokine, with 10 ng/mL Hyper-IL-6 or with 10 ng/mL Hyper-IL-6 and 100 ng/mL 3xGFP-Fc or 3xmCherry-Fc. Error bars indicate S.D., p value was determined using two-way ANOVA ***, $p < 0.001$; *, $p < 0.1$.

(C) Proliferation of Ba/F3/gp130 and Ba/F3/gp130/G_{VHH}Fas cells incubated without cytokine, with 10 ng/mL Hyper-IL-6 or with 10 ng/mL Hyper-IL-6 and GFP, GFP-Fc, 3xGFP-Fc or GFP_3. Error bars indicate S.D., p value was determined using two-way ANOVA ***, $p < 0.001$.

(D) Schematic illustration of $mCherry_{VHH}$Fas (red, blue) and $mCherry_{VHH}Fas_{E256G}$ (yellow star). Created with BioRender.com.

(E) Proliferation of Ba/F3/gp130 and Ba/F3/gp130/$C_{VHH}Fas_{E256G}$ cells incubated without cytokine, with 10 ng/mL Hyper-IL-6 or with 10 ng/mL Hyper-IL-6 and 100 ng/mL mCherry-Fc or 3xmCherry-Fc. Error bars indicate S.D., p value was determined using two-way ANOVA ***, $p < 0.001$. (B, C, E) One representative experiment out of three is shown.

98.3% (GFP_3), 98.8% (3xmCherry-Fc), 99.0% ($mCherry_3$) of the cells were in late apoptosis (Tables 1 and 2, Figures S8A andS8B). This indicates that dimeric synthetic Fas stimulation induced apoptosis albeit to a lesser and slower extent compared to trimeric or hexameric Fas stimulation. Taken together, we have shown that activation of synthetic Fas efficiently induced cellular apoptosis.

Simultaneous functional integration of pro- and anti-apoptotic synthetic cytokine receptors for IL-6 and Fas-signaling

Finally, we combined the apoptotic C_{VHH}Fas with the recently described anti-apoptotic/proliferative synthetic cytokine receptor G_{VHH}gp130 which phenocopied IL-6 signaling (Mossner et al., 2020b) (Figure S9A) to enable the switch from gp130-mediated proliferation into Fas-mediated apoptosis (Figure 4A). Cell surface expression of G_{VHH}gp130 and C_{VHH}Fas in Ba/F3/gp130 cells was shown by flow cytometry (Figure S9B) and proliferation of Ba/F3/G_{VHH}gp130/C_{VHH}Fas was specifically induced by dimeric GFP-Fc (Figure 4B). Co-stimulation of these cells with GFP-Fc and 3xmCherry-Fc resulted in complete abrogation of cellular proliferation. EC_{50} for induction of cellular proliferation mediated by GFP-Fc via G_{VHH}gp130 was 7.5 ng/mL (Figure 4C), whereas the IC_{50} for abrogation of cellular proliferation mediated by 3xmCherry-Fc via C_{VHH}Fas was 0.27 ng/mL (247.7 pM) and 0.11 ng/mL (13.4 pM) for $mCherry_3$ (Figure 4C). Stimulation with GFP-Fc induced pSTAT3, co-incubation with 3xmCherry-Fc or $mCherry_3$ resulted in Caspase 3 activation and downregulation of pSTAT3 (Figure 4D). Finally, Ba/F3/gp130/G_{VHH}gp130/C_{VHH}Fas cells were stimulated for 24 and 48 hr with GFP-Fc in the presence and absence of 3xmCherry-Fc or $mCherry_3$ and apoptosis was monitored by Annexin V and 7-AAD staining. Ba/F3/gp130/G_{VHH}gp130/C_{VHH}Fas cells incubated for 24 hr with Hyper-IL-6 or GFP-Fc were alive to 94.7% or 89.8%, whereas 70% EtOH killed 99.3% of the cells (Table 3, Figure S10A). As expected, co-stimulation of GFP-Fc and 3xmCherry-Fc or $mCherry_3$ resulted in 92.7% or 94.8% late apoptotic cells, respectively. After 48 hr there was no difference between cells incubated with Hyper-IL-6 or GFP-Fc 85.7% and 83.4%. Co-incubation of GFP-Fc with 3xmCherry-Fc or $mCherry_3$ resulted in 92.8% and 93.1% cells in the late apoptotic phase (Table 3, Figure S10B). Our data showed that two synthetic cytokine receptors with pro- and anti-apoptotic functions can be combined in a single cell to confer opposite cellular reactions.

DISCUSSION

The SyCyR system belongs to a new class of fully synthetic cytokine systems combining synthetic ligands and synthetic receptors (Scheller et al., 2019). Until now, the SyCyR system was adopted to classical dimeric cytokine receptor families for IL-6, IL-23, or IL-22 (Engelowski et al., 2018; Mossner et al., 2020a, 2020b). To date, synthetic systems such as chimeric receptors or synthekines were limited to the analysis of dimeric receptor combinations (Floss et al., 2017; Moraga et al., 2017). Here, we established the first synthetic trimeric cytokine receptor assembly for receptors of the TNFRSF. IκB phosphorylation as marker for the activation of the NF-κB signaling pathway revealed that TNFR1-and TNFR2-SyCyRs were, however, activated as homotrimers or homo-hexamers but not as heterotrimers and homodimers. While the TNFR1 can be activated by soluble (sTNFα) and membrane bound (mTNFα) TNFα, the TNFR2 is mainly activated by mTNFα (Cabal-Hierro and Lazo, 2012), albeit our synthetic TNFR2 was also activated by synthetic soluble ligands. Both receptors comprise signaling form survival to cell death and their dysregulation is often linked to various diseases (Dostert et al., 2019). The investigation of the death receptor SyCyRs for Fas, TrailR1, and TrailR2 showed that only the Fas-SyCyR efficiently activated apoptosis regardless of the utilized nanobody. Basically, there were only subtle differences in the outcome between the activation as trimeric or hexameric receptors. These differences were shown in the Western blot analysis after 6 hr of cell stimulation. Cells stimulated with the trimeric ligands already showed complete cleavage of pro-Caspase 3 whereas cells stimulated with hexameric ligands only showed a reduction in pro-Caspase 3. The circular arrangement of the trimeric GFP_3 and $mCherry_3$ probably induces apoptosis faster because the receptors are closer to

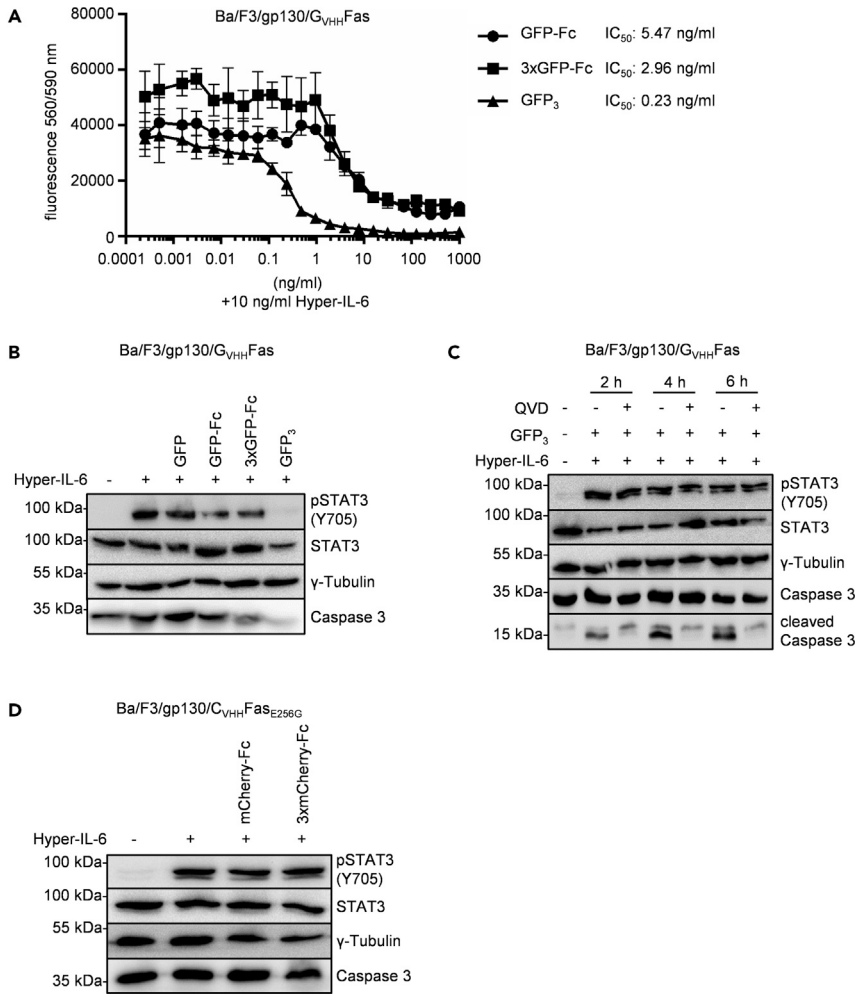

Figure 3. Characterization of Fas-SyCyRs

(A) Proliferation of Ba/F3/gp130/G_{VHH}Fas cells incubated with increasing concentrations of GFP-Fc, 3xGFP-Fc or GFP_3 from 0.0001–1000 ng/mL and 10 ng/mL Hyper-IL-6. Error bars indicate S.D.

(B) Activation of Caspase 3 and STAT3 activation of Ba/F3/gp130/G_{VHH}Fas cells stimulated without cytokine, with 10 ng/mL Hyper-IL-6 or 10 ng/mL Hyper-IL-6 and 100 ng/mL GFP, GFP-Fc, 3xGFP-Fc, GFP_3 for 6 hr. Equal amounts of protein (50 μg/lane) were analyzed via specific antibodies detecting Caspase 3, γ-Tubulin, phospho-STAT3 or STAT3.

(C) Time dependent activation and inhibition of Caspase 3 in Ba/F3/gp130/G_{VHH}Fas cells stimulated without cytokine or with 100 ng/mL GFP_3 and 10 ng/mL Hyper-IL-6 for 2, 4 or 6 hr. For each time point cells were once incubated without and once with 10 μM of the Caspase inhibitor QVD. Equal amounts of protein (50 μg/lane) were analyzed via specific antibodies detecting Caspase 3, γ-Tubulin, phospho-STAT3 or STAT3.

(D) Cleavage of Caspase 3 and STAT3 activation of Ba/F3/gp130/$C_{VHH}Fas_{E256G}$ cells stimulated without cytokine, with 10 ng/mL Hyper-IL-6 or 10 ng/mL Hyper-IL-6 and 100 ng/mL mCherry-Fc or 3xmCherry-Fc for 6 hr. Equal amounts of protein (50 μg/lane) were analyzed via specific antibodies detecting Caspase 3, γ-Tubulin, phospho-STAT3 or STAT3. (A-D) One representative experiment out of three is shown.

each other and mimic the endogenous activation of Fas better. This difference in the activation is only detectable within the first few hours since the Annexin V/7-AAD staining after 24 hr showed no difference between these two types of ligands. Surprisingly, also an activation as dimer induced Fas-mediated apoptosis. Here, we could see that apoptosis induced by FasL dimers is carried out slower than apoptosis of trimeric or hexameric FasL. Recent studies showed that Fas receptors are arranged as antiparallel dimers that form overall hexagonal lattices without the ligand (Vanamee and Faustman, 2018a; Vanamee and Faustman, 2020). This arrangement is necessary for the appropriate DISC formation and interaction with FADD upon ligand binding. The binding of the ligand thereby shifts the equilibrium of the Fas death domain from the closed to the open state (Scott et al., 2009). Two adjacent Fas receptors then form Fas-Fas bridges that stabilize this open form and enable the binding of FADD (Scott et al.,

Table 1. Analysis of apoptosis progression in Ba/F3/gp130/G_{VHH}Fas cells

	24 hr		48 hr	
Ba/F3/gp130/G_{VHH}Fas	Alive	Apoptosis	Alive	Apoptosis
Hyper-IL-6	93.7	5.12	87.6	4.09
EtOH + Hyper-IL-6	0.42	99.0	0.28	97.3
GFP + Hyper-IL-6	87.1	5.61	54.6	4.03
GFP-Fc + Hyper-IL-6	62.1	31.7	28.8	63.9
3xGFP-Fc + Hyper-IL-6	4.83	92.3	3.62	95.4
GFP_3 + Hyper-IL-6	1.26	94.0	0.99	98.3

Ba/F3/gp130/G_{VHH}Fas cells were incubated for 24 hr or 48 hr with 10 ng/mL Hyper-IL-6 or 10 ng/mL Hyper-IL-6 and 100 ng/mL GFP, GFP-Fc, 3xGFP-Fc or GFP_3. For the condition EtOH +10 ng/mL Hyper-IL-6 cells were incubated only with Hyper-IL-6 for the indicated time points and washed with 70% EtOH before the measurement. Cells were stained with Annexin V and 7-AAD and analysis was carried out using flow cytometry.

2009). Since these hydrophobic interactions are rather weak Fas-Fas dimers tend to form tetramers or higher ordered oligomers (Scott et al., 2009). Nevertheless, these dimers can be sufficient for the activation of the downstream Caspase cascade. The binding of FADD to the death domain of Fas recruits pro-Caspase 8, which can be auto-activated by dimerization (Shen et al., 2018). Although dimerization is sufficient for the activation, higher ordered oligomers stabilize and speed up the whole process (Shen et al., 2018). This indicates that although the activation of Fas is naturally mediated via trimeric ligands and favors oligomeric receptor assemblies, Fas also has the potential to be activated as dimer. In addition, the stoichiometry of the TNFR–TNF binding sites was investigated using TNFR-Fas chimeras (Boschert et al., 2010). Generating TNF with only one or two receptor binding sites, they showed that the TNFR-Fas chimera can also be activated as dimer (Boschert et al., 2010). With our synthetic system we were able to investigate this possibility further and indeed we could show active Fas dimers. The induction of apoptosis by the Fas-SyCyR dimer is slower than for the trimeric or oligomeric Fas-SyCyR, which is in line with the findings of Scott et al., (2009) and Shen et al., (2018). Since the Fas-SyCyRs were modified on the extracellular site, there is no pre-assembly as antiparallel dimer. However, the distance between SyCyRs upon ligand binding seems to enable the formation of Fas-Fas bridges that stabilize each other and facilitate DISC formation. The specificity of induced apoptosis due to the synthetic Fas activation was verified by a loss-of-function mutation in the death domain leading to no apoptosis upon activation of the mutated Fas-SyCyR. Patient mutations of the Fas death domain are associated with the development of autoimmune lymphoproliferative syndrome (ALPS) (F. Rieux-Laucat et al., 1995), but only a limited number of single nucleotide polymorphisms (SNPs) have been functionally characterized (Price et al., 2014; Tauzin et al., 2012). Most mutations are heterozygous since homozygote mutations are typically lethal (Fisher et al., 1995). Application of the SyCyR system could facilitate the analysis of these mutations on the one hand as homo- or on the other hand as heterotrimer with the functional Fas-SyCyR. With increasing sequencing data and the expansion of personalized medicine the number of known SNPs will probably rise exponentially. Facing this, new systems like the SyCyR approach may allow efficient biochemical analysis. Usage of two independent SyCyRs in one cell demonstrates possible combinatory applicability for

Table 2. Analysis of apoptosis progression in Ba/F3/gp130/C_{VHH}Fas cells

	24 hr		48 hr	
Ba/F3/gp130/C_{VHH}Fas	Alive	Apoptosis	Alive	Apoptosis
Hyper-IL-6	84.7	10.5	87.7	5.80
EtOH + Hyper-IL-6	0.26	98.9	0.63	93.8
mCherry + Hyper-IL-6	84.7	10.4	89.6	4.11
mCherry-Fc + Hyper-IL-6	75.8	18.0	53.2	40.5
3xmCherry-Fc + Hyper-IL-6	35.6	62.2	0.65	98.8
$mCherry_3$ + Hyper-IL-6	28.9	70.1	0.38	99.0

Ba/F3/gp130/C_{VHH}Fas cells were incubated for 24 hr or 48 hr with 10 ng/mL Hyper-IL-6 or 10 ng/mL Hyper-IL-6 and 100 ng/mL mCherry, mCherry-Fc, 3xmCherry-Fc or $mCherry_3$. For the condition EtOH +10 ng/mL Hyper-IL-6 cells were incubated only with Hyper-IL-6 for the indicated time points and washed with 70% EtOH before the measurement. Cells were stained with AnnexinV and 7-AAD and analysis was carried out using flow cytometry.

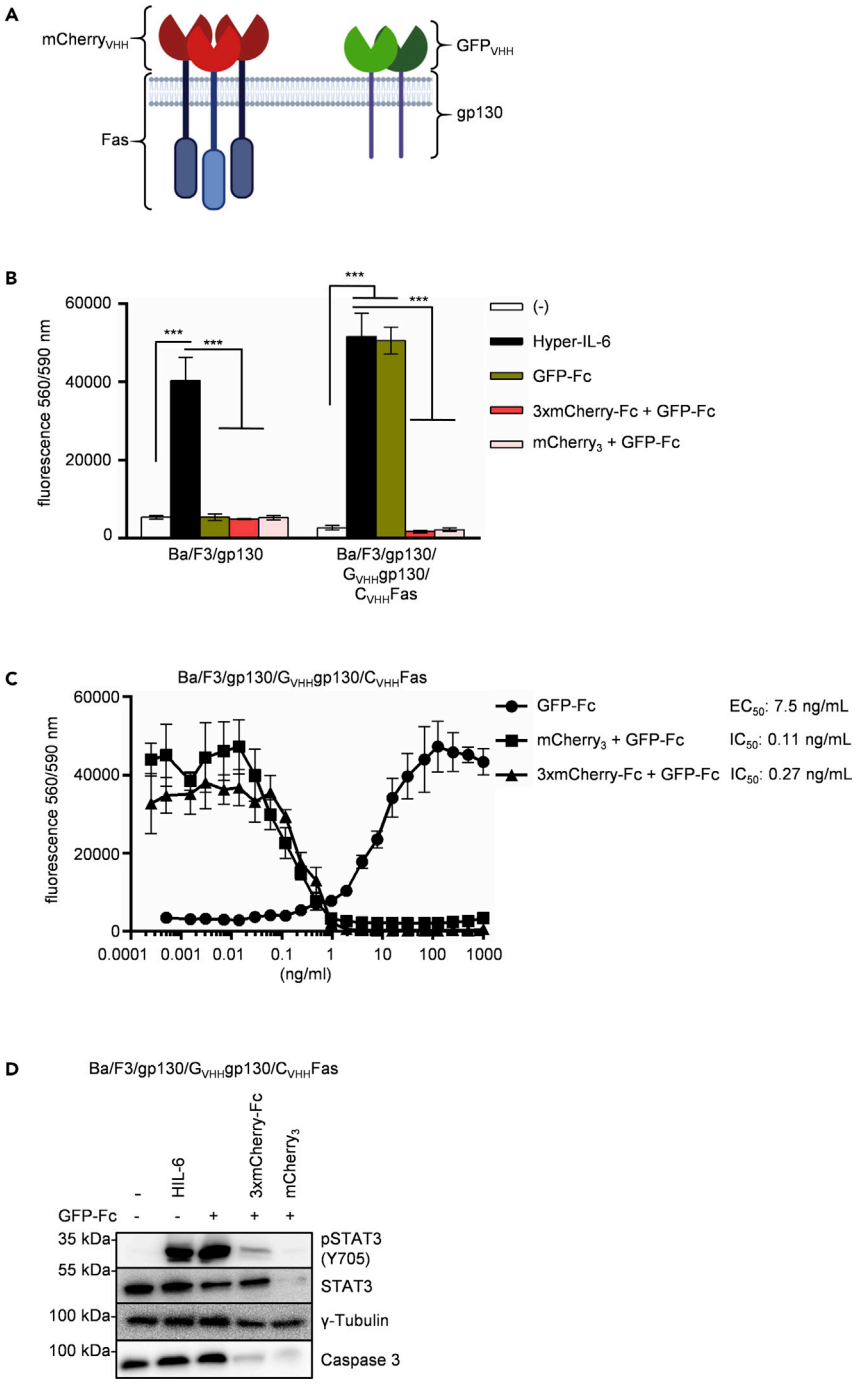

Figure 4. Simultaneous functional integration of pro- and anti-apoptotic synthetic cytokine receptors for IL-6 and Fas-signaling

(A) Schematic illustration of mCherry$_{VHH}$Fas (red, blue) and GFP$_{VHH}$gp130 (green, purple) in one cell. Created with BioRender.com.

(B) Proliferation of Ba/F3/gp130 and Ba/F3/gp130/GFP$_{VHH}$gp130/mCherry$_{VHH}$Fas cells incubated without cytokine, with 10 ng/mL Hyper-IL-6, with 100 ng/mL GFP-Fc or with 100 ng/mL GFP-Fc and 100 ng/mL 3xmCherry-Fc or mCherry$_3$. Error bars indicate S.D., p value was determined using two-way ANOVA ***, $p < 0.001$.

(C) Ba/F3/gp130/GFP$_{VHH}$gp130/mCherry$_{VHH}$Fas cells were incubated with increasing concentrations of GFP-Fc, mCherry$_3$ or 3xmCherry-Fc from 0.001–1000 ng/mL. mCherry$_3$ and 3xmCherry-Fc conditions were supplemented with 100 ng/mL GFP-Fc. Error bars indicate S.D.

Figure 4. *Continued*

(D) Cleavage of Caspase 3 and STAT3 activation of Ba/F3/gp130/G_{VHH}gp130/C_{VHH}Fas cells stimulated without cytokine, with 10 ng/mL Hyper-IL-6, with 100 ng/mL GFP-Fc or 100 ng/mL GFP-Fc and 100 ng/mL 3xmCherry-Fc or $mCherry_3$ for 6 hr. Equal amounts of protein (50 μg/lane) were analyzed via specific antibodies detecting Caspase 3, γ-Tubulin, phospho-STAT3 or STAT3. (B–D) One representative experiment out of three is shown.

the SyCyR system. Depending on which receptor was activated, cells either proliferated via gp130-SyCyR or went into apoptosis via Fas-SyCyR, again showing the specificity of the system. Overall, the modular system of the synthetic GFP and mCherry ligands allows an exact homo- or hetero-composition of up to six receptors to allow tailor-made activation of natural or non-natural receptor combinations. This possibility might be useful to support CAR-T-cell therapies (June et al., 2018) with tailor-made SyCyRs either assisting or repressing the activity of CAR-T-cells. Currently, research is focused on the improvement of the CAR-T-cell therapy safety and their application for solid tumors by using synthetic circuits (Caliendo et al., 2019). CARs are modified with kill switches to eliminate the CAR-T-cells in case of severe toxicities or to improve the tumor specific activation with switchable CAR-T-cells (Caliendo et al., 2019). The synthetic Notch (synNotch) receptor approach seems to be an ideal tool for this since they can be engineered to have extracellular sensors which upon stimulation can specifically influence transcription (Williams et al., 2020; Roybal and Lim, 2017). T-cells with synNotch receptors have already shown a robust and highly controlled custom behavior with the ability to induce the expression of antibodies, cytokines, or therapeutic proteins (Bonfa et al., 2020; Roybal et al., 2016). A combined approach of the synNotch and SyCyR system could use the synNotch receptor as sensor for cellular stress or disease markers, inducing transcription of the synthetic ligand. The ligand would then only activate the SyCyRs if conditional changes of the cellular environment require the activation of specific SyCyRs. Here, synNotch receptors detecting different markers could be used to either activate pro- or anti-apoptotic SyCyRs. This SyCyR activation would probably be faster and more sensitive than external ligand application after changes in the patient's condition have been detected. Cytokines also harbor the potential to limit tumor growth but due to their redundancy and short half-life their application is difficult (Bonfa et al., 2020). The SyCyR system opens up new pathways of their application since due to its specificity there are no more off-target activations and the signaling can be regulated nicely via the synthetic ligand application. Additionally, boosting of CAR-T-cells via SyCyRs may help to overcome the current limitations in the CAR-T-cell treatment of solid tumors (Bonfa et al., 2020).

Limitations of the study

As shown and discussed before, this study shows early research into the usage of a new synthetic cytokine system. Further studies are necessary to verify these findings *in vivo* and to analyze the potential combination with the CAR-T-cell treatment.

STAR★METHODS

Detailed methods are provided in the online version of this paper and include the following:

- KEY RESOURCES TABLE
- RESOURCE AVAILABILITY
  - Lead contact
  - Materials availability

Table 3. Analysis of apoptosis progression in Ba/F3/gp130/G_{VHH}gp130/C_{VHH}Fas cells

	24 hr		48 hr	
Ba/F3/gp130/G_{VHH}gp130/C_{VHH}Fas	Alive	Apoptosis	Alive	Apoptosis
Hyper-IL-6	94.7	3.58	85.7	4.02
GFP-Fc	89.8	5.43	83.4	5.48
EtOH + GFP-Fc	0.49	99.3	0.56	98.4
3xmCherry-Fc + GFP-Fc	2.62	92.7	2.71	92.8
$mCherry_3$ + GFP-Fc	2.77	94.8	1.9	93.1

Apoptosis progression by analysis of Annexin V and 7-AAD staining of Ba/F3/gp130/G_{VHH}gp130/C_{VHH}Fas cells incubated for 24 hr or 48 hr with 10 ng/mL Hyper-IL-6, 100 ng/mL GFP-Fc or 100 ng/mL GFP-Fc and 100 ng/mL 3xmCherry-Fc or $mCherry_3$. For the condition EtOH +100 ng/mL GFP-Fc cells were incubated only with GFP-Fc for the indicated time points and washed with 70% EtOH before the measurement. Analysis was carried out using flow cytometry.

SUPPLEMENTAL INFORMATION

Supplemental information can be found online at https://doi.org/10.1016/j.isci.2021.102471.

ACKNOWLEDGMENTS

We thank Petra Oprée for assistance. The study was supported by grants from Deutsche Forschungsgemeinschaft (DFG SCHE 907/5-1).

AUTHOR CONTRIBUTIONS

S.M. conducted all experiments, analyzed the data, and wrote the paper. D.M.F. helped develop the experiments. J.S. designed the study, analyzed the data, and wrote the paper.

DECLARATION OF INTERESTS

The authors declare no competing interests.

Received: February 2, 2021
Revised: March 30, 2021
Accepted: April 22, 2021
Published: May 21, 2021

REFERENCES

Aggarwal, B.B. (2003). Signalling pathways of the TNF superfamily: a double-edged sword. Nat. Rev. Immunol. *3*, 745–756.

Bodmer, J.-L., Schneider, P., and Tschopp, J. (2002). The molecular architecture of the TNF superfamily. Trends Biochem. Sci. *27*, 19–26.

Bonfa, G., Blazquez-Roman, J., Tarnai, R., and Siciliano, V. (2020). Precision tools in immuno-oncology: synthetic gene circuits for cancer immunotherapy. Vaccines (Basel) *8*, 732.

Boschert, V., Krippner-Heidenreich, A., Branschadel, M., Tepperink, J., Aird, A., and Scheurich, P. (2010). Single chain TNF derivatives with individually mutated receptor binding sites reveal differential stoichiometry of ligand receptor complex formation for TNFR1 and TNFR2. Cell Signal. *22*, 1088–1096.

Brenner, D., Blaser, H., and Mak, T.W. (2015). Regulation of tumour necrosis factor signalling: live or let die. Nat. Rev. Immunol. *15*, 362–374.

Cabal-Hierro, L., and Lazo, P.S. (2012). Signal transduction by tumor necrosis factor receptors. Cell Signal. *24*, 1297–1305.

Caliendo, F., Dukhinova, M., and Siciliano, V. (2019). Engineered cell-based therapeutics: synthetic biology meets immunology. Front.Bioeng.Biotechnol. *7*, 43.

Chakravarti, D., and Wong, W.W. (2015). Synthetic biology in cell-based cancer immunotherapy. Trends Biotechnol. *33*, 449–461.

Chinnaiyan, A.M., O'Rourke, K., Tewari, M., and Dixit, V.M. (1995). FADD, a novel death domain-containing protein, interacts with the death domain of fas and initiates apoptosis. Cell *81*, 505–512.

Creagh, E.M., and Martin, S.J. (2001). Caspases: cellular demolition experts. Biochem. Soc. Trans. *29*, 696–702.

Dempsey, P.W., Doyle, S.E., He, J.Q., and Cheng, G. (2003). The signaling adaptors and pathways activated by TNF superfamily. Cytokine Growth Factor Rev. *14*, 193–209.

Dostert, C., Grusdat, M., Letellier, E., and Brenner, D. (2019). The TNF family of ligands and receptors: communication modules in the immune system and beyond. Physiol. Rev. *99*, 115–160.

Engelowski, E., Schneider, A., Franke, M., Xu, H., Clemen, R., Lang, A., Baran, P., Binsch, C., Knebel, B., Al-Hasani, H., et al. (2018). Synthetic cytokine receptors transmit biological signals using artificial ligands. Nat. Commun. *9*, 2034.

Faustman, D., and Davis, M. (2010). TNF receptor 2 pathway: drug target for autoimmune diseases. Nat. Rev. Drug Discov. *24*, 482–493.

Fazel Modares, N., Polz, R., Haghighi, F., Lamertz, L., Behnke, K., Zhuang, Y., Kordes, C., Haussinger, D., Sorg, U.R., Pfeffer, K., et al. (2019). IL-6 trans-signaling controls liver regeneration after partial hepatectomy. Hepatology *70*, 2075–2091.

Fischer, M., Goldschmitt, J., Peschel, C., Brakenhoff, J.P., Kallen, K.J., and Wollmer, A. (1997). A bioactive designer cytokine for human

hematopoietic progenitor cell expansion. Nat. Biotechnol. *15*, 142–145.

Fisher, G.H., Rosenberg, F.J., Straus, S.E., Dale, J.K., Middelton, L.A., Lin, A.Y., Strober, W., Lenardo, M.J., and Puck, J.M. (1995). Dominant interfering fas gene mutations impair apoptosis in a human autoimmune lymphoproliferative syndrome. Cell *81*, 935–946.

Floss, D.M., Mrotzek, S., Klocker, T., Schroder, J., Grotzinger, J., Rose-John, S., and Scheller, J. (2013). Identification of canonical tyrosine-dependent and non-canonical tyrosine-independent STAT3 activation sites in the intracellular domain of the interleukin 23 receptor. J. Biol. Chem. *288*, 19386–19400.

Floss, D.M., Schonberg, M., Franke, M., Horstmeier, F.C., Engelowski, E., Schneider, A., Rosenfeldt, E.M., and Scheller, J. (2017). IL-6/IL-12 cytokine receptor shuffling of extra- and intracellular domains reveals canonical STAT activation via synthetic IL-35 and IL-39 signaling. Sci. Rep. *7*, 15172.

Fridy, P.C., Li, Y., Keegan, S., Thompson, M.K., Nudelman, I., Scheid, J.F., Oeffinger, M., Nussenzweig, M.C., Fenyo, D., Chait, B.T., et al. (2014). A robust pipeline for rapid production of versatile nanobody repertoires. Nat. Methods *11*, 1253–1260.

Grakoui, A., Bromley, S.K., Sumen, C., Davis, M.M., Shaw, A.S., Allen, P.M., and Dustin, M.L. (1999). The immunological synapse: a molecular machine controlling T cell activation. Science *285*, 221.

June, C., O'Connor, R., Kawalekar, O., Ghassemi, S., and Milone, M. (2018). CAR T cell immunotherapy for human cancer. Science *359*, 1361–1365.

Ketteler, R., Moghraby, C., Hsiao, J., Sandra, O., Lodish, H., and Klingmüller, U. (2003). The cytokine-inducible Scr homology domain-containing protein negatively regulates signaling by promoting apoptosis in erythroid progenitor cells. J. Biol. Chem. *278*, 2654–2660.

Lin, Y., Bai, L., Chen, W., and Xu, S. (2010). The NF-kappaB activation pathways, emerging molecular targets for cancer prevention and therapy. Expert Opin.Ther. Targets *14*, 45–55.

Locksley, R.M., Killeen, N., and Lenardo, M.J. (2001). The TNF and TNF receptor superfamilies: integrating mammalian biology. Cell *104*, 487–501.

McIlwain, D.R., Berger, T., and Mak, T.W. (2015). Caspase functions in cell death and disease. Cold Spring Harb.Perspect.Biol. *7*, a026716.

Moraga, I., Spangler, J.B., Mendoza, J.L., Gakovic, M., Wehrman, T.S., Krutzik, P., and Garcia, K.C. (2017). Synthekines are surrogate cytokine and growth factor agonists that compel signaling through non-natural receptor dimers. Elife *6*, e22882.

Mossner, S., Kuchner, M., Fazel Modares, N., Knebel, B., Al-Hasani, H., Floss, D.M., and Scheller, J. (2020a). Synthetic interleukin 22 (IL-22) signaling reveals biological activity of homodimeric IL-10 receptor 2 and functional cross-talk with the IL-6 receptor gp130. J. Biol. Chem. *295*, 12378–12397.

Mossner, S., Phan, H., Triller, S., Moll, J., Conrad, U., and Scheller, J. (2020b). Multimerization strategies for efficient production and purification of highly active synthetic cytokine receptor ligands. PLoS One *15*, e0230804.

Orlinick, J.R., Vaishnaw, A., Elkon, K.B., and Chao, M.V. (1997). Requirement of cysteine-rich repeats of the fas receptor for binding by the fas ligand*. J. Biol. Chem. *272*, 28889–28894.

Peters, A.M.J., Kohfink, B., Martin, H., Frank, G., Wörmann, B., Gahr, M., and Roesler, J. (1999). Defective apoptosis due to a point mutation in the death domain of CD95 associated with autoimmune lymphoproliferative syndrome, T-cell lymphoma, and Hodgkin's disease. Exp. Hematol. *27*, 868–874.

Porter, A.G., and Ru, J. (1999). Emerging roles of caspase-3 in apoptosis. Cell Death Differ. *6*, 99–104.

Price, S., Shaw, P.A., Seitz, A., Joshi, G., Davis, J., Niemela, J.E., Perkins, K., Hornung, R.L., Folio, L., Rosenberg, P.S., et al. (2014). Natural history of autoimmune lymphoproliferative syndrome associated with FAS gene mutations. Blood *123*, 1989–1999.

Rieux-Laucat, F., Le Deist, F., Hivroz, C., Roberts, A.G., Debatin, K.M., Fischer, A., and Villartay, J.P.D. (1995). Mutations in fas associated with human lymphoproliferative syndrome and autoimmunity. Science *268*, 1347–1349.

Rothbauer, U., Zolghadr, K., Muyldermans, S., Schepers, A., Cardoso, M.C., and Leonhardt, H. (2008). A versatile nanotrap for biochemical and functional studies with fluorescent fusion proteins. Mol. Cell Proteomics *7*, 282–289.

Roybal, K.T., Williams, J.Z., Morsut, L., Rupp, L.J., Kolinko, I., Choe, J.H., Walker, W.J., McNally, K.A., and Lim, W.A. (2016). Engineering T cells with customized therapeutic response programs using synthetic Notch receptors. Cell *167*, 419–432 e416.

Roybal, K.T., and Lim, W.A. (2017). Synthetic immunology: hacking immune cells to expand their therapeutic capabilities. Annu. Rev. Immunol. *35*, 229–253.

Savic, S., Dickie, L.J., Battellino, M., and McDermott, M.F. (2012). Familial Mediterranean fever and related periodic fever syndromes/autoinflammatory diseases. Curr.Opin.Rheumatol. *24*, 103–112.

Scheller, J., Engelowski, E., Moll, J.M., and Floss, D.M. (2019). Immunoreceptor engineering and synthetic cytokine signaling for therapeutics. Trends Immunol. *40*, 258–272.

Schmitz, J., Weissenbach, M., Haan, S., Heinrich, P.C., and Schaper, F. (2000). SOCS3 exerts its inhibitory function on interleukin-6 signal transduction through the SHP2 recruitment site of gp130. J. Biol. Chem. *275*, 12848–12856.

Scott, F.L., Stec, B., Pop, C., Dobaczewska, M.K., Lee, J.J., Monosov, E., Robinson, H., Salvesen, G.S., Schwarzenbacher, R., and Riedl, S.J. (2009). The Fas-FADD death domain complex structure unravels signalling by receptor clustering. Nature *457*, 1019–1022.

Shen, C., Pei, J., Guo, X., Zhou, L., Li, Q., and Quan, J. (2018). Structural basis for dimerization of the death effector domain of the F122A mutant of Caspase-8. Sci. Rep. *8*, 16723.

Shishodia, S., and BB, A. (2004). Nuclear factor-kappaB: a friend or a foe in cancer? Biochem.Pharmacol. *68*, 1071–1080.

Si, W., Li, C., and Wei, P. (2018). Synthetic immunology: T-cell engineering and adoptive immunotherapy. Synth. Syst. Biotechnol. *3*, 179–185.

Starling, G.C., Bajorath, J., Emswiler, J., Ledbetter, J.A., Aruffo, A., and Kiener, P.A. (1997). Identification of amino acid residues important for ligand binding to fas. J. Exp. Med. *185*, 1487–1492.

Suthaus, J., Tillmann, A., Lorenzen, I., Bulanova, E., Rose-John, S., and Scheller, J. (2011). Forced homo- and heterodimerization of all gp130-type receptor complexes leads to constitutive ligand-independent signaling and cytokine-independent growth. Mol. Biol. Cell *21*, 797–2807.

Tauzin, S., Debure, L., Moreau, J.-F., and Legembre, P. (2012). CD95-mediated cell signaling in cancer: mutations and post-translational modulations. Cell Mol. Life Sci. *69*, 1261–1277.

Vanamee, É.S., and Faustman, D.L. (2018a). Structural principles of tumor necrosis factor superfamily signaling. Sci. Signal. *11*, eaao4910.

Vanamee, É.S., and Faustman, D.L. (2018b). Structural principles of tumor necrosis factor superfamily signaling. Sci. Signal. *11*, eaao4910.

Vanamee, E.S., and Faustman, D.L. (2020). On the TRAIL of better therapies: understanding TNFRSF structure-function. Cells *9*, 764.

Wesolowski, J., Alzogaray, V., Reyelt, J., Unger, M., Juarez, K., Urrutia, M., Cauerhff, A., Danquah, W., Rissiek, B., Scheuplein, F., et al. (2009). Single domain antibodies: promising experimental and therapeutic tools in infection and immunity. Med. Microbiol. Immunol. *198*, 157–174.

Williams, J.Z., Allen, G.M., Shah, D., Sterin, I.S., Kim, K.H., Garcia, V.P., Shavey, G.E., Yu, W., Puig-Saus, C., Tsoi, J., et al. (2020). Precise T cell recognition programs designed by transcriptionally linking multiple receptors. Science *370*, 1099–1104.

Wilson, N.S., Dixit, V., and Ashkenazi, A. (2009). Death receptor signal transducers: nodes of coordination in immune signaling networks. Nat. Immunol. *10*, 348–355.

STAR★METHODS

KEY RESOURCES TABLE

REAGENT or RESOURCE	SOURCE	IDENTIFIER
Antibodies		
Phospho-STAT3 (Tyr705, D3A7)	Cell Signaling Technology	Cat# 9145, RRID:AB_2491009
STAT3 (124H6)	Cell Signaling Technology	Cat# 9139, RRID:AB_331757
Caspase-3 (8G10)	Cell Signaling Technology	Cat# 9665, RRID:AB_2069872
pIκB (Ser23; 14D4)	Cell Signaling Technology	cat. #2859
HA-Tag (C29F4)	Cell Signaling Technology	Cat# 3724, RRID:AB_1549585
Bacterial and virus strains		
Escherichia coli XL1-Blue	Agilent Technology	cat. # 200249
Biological samples		
Chemicals, peptides, and recombinant proteins		
TurboFect	Thermo Fisher Scientific	cat. #R0532
Polybrene	Sigma-Aldrich	TR-1003-G
Puromycin	Carl Roth	cat. #0240.1
Hygromycin B	Carl Roth	cat. #1287.2
7-AAD	R&D Systems	cat. #7121/1
Critical commercial assays		
CellTiter-Blue Viability Assay	Promega	cat. #G808A
Experimental models: cell lines		
Ba/F3/gp130	Immunex	N/A
Phoenix-Eco	Ursula Klingmüller, DKFZ	N/A
Oligonucleotides		
GAPDH: fw 5′: GAAGGGCTCATGACCACAGT, rev 5′: CATTGTCATACCAGGAAATGAGCT	This paper	N/A
FasL: fw 5′: GCGGGTTCGTGAAACTGATAA, rev 5′: GCAAAATGGGCCTCCTTGATA	This paper	N/A
Traf1: fw 5′: AGGGTGGTGGAATTACAGCAA, rev 5′: GCAGTGTAGAAAGCTGGAGAG	This paper	N/A
IL-6: fw 5′: CAAAGCCAGAGTCCTTCAGA, rev 5′: GATGGTCTTGGTCCTTAGCC	This paper	N/A
TNFα: fw 5′: CTGAACTTCGGGGTGATCGG, rev 5′: GGCTTGTCACTCGAATTTTGAGA	This paper	N/A
Recombinant DNA		
Fas	BioCat	N/A
TrailR1	BioCat	N/A
TrailR2	BioCat	N/A
Software and algorithms		
GraphPad Prism 6	GraphPad Software	

RESOURCE AVAILABILITY

Lead contact

Further information and requests for resources and reagents should be directed to and will be fulfilled by the lead contact, Jürgen Scheller (jscheller@uni-duesseldorf.de).

Materials availability

This study did not generate new unique reagents. All cDNAs are available upon request.

Data and code availability

Sequence data are shown in the supplementary tables.

EXPERIMENTAL MODEL AND SUBJECT DETAILS

Cell lines

Murine Ba/F3/gp130 cells were obtained from Immunex (Seattle, WA, USA). Phoenix-Eco cells were received from Ursula Klingmüller (DKFZ, Heidelberg, Germany). Cells were grown at 37°C with 5% CO_2 in Dulbecco's Modified Eagle's high glucose culture medium (DMEM) from GIBCO (Life Technologies, Darmstadt, Germany). The medium was supplemented with 10% fetal calf serum from GIBCO(Life Technologies, Darmstadt, Germany), 60 mg/l penicillin and 100 mg/l streptomycin from Genaxxon (Bioscience GmbH, Ulm, Germany).

METHOD DETAILS

Cells and reagents

All cells were grown at 37°C with 5% CO_2 in a water saturated atmosphere in Dulbecco's modified Eagle's Medium (DMEM) high glucose culture medium (GIBCO®, Life Technologies, Darmstadt, Germany) with 10% fetal calf serum (GIBCO®, Life Technologies, Darmstadt, Germany) and 60 mg/l penicillin and 100 mg/l streptomycin (Genaxxon Bioscience GmbH, Ulm, Germany). Murine Ba/F3/gp130 cells were obtained from Immunex (Seattle, WA, USA) and grown in the presence of Hyper-IL-6, a fusion protein of IL-6 and soluble IL-6 receptor (Fischer et al., 1997). 0.2% (10 ng/ml) of conditioned medium from a stable clone of CHO-K1 cells secreting Hyper-IL-6 in the supernatant (stock solution approximately 10 µg/ml as determined by ELISA) were used to maintain Ba/F3/gp130 cells and derivates thereof. The packaging cell line Phoenix-Eco was received from Ursula Klingmüller (DKFZ, Heidelberg, Germany). Phospho-STAT3 (Tyr705; D3A7; cat.#9145; 1:1000), STAT3 (124H6; cat.#9139; 1:1000), Caspase-3 (8G10; cat.#9662; 1:1000), pIκB (Ser23; 14D4; cat.#2859; 1:1000), IκB (44D4; cat.#4812; 1:1000), GFP (4B10; cat.#2955; 1:1000), Myc-Tag (71D10; cat.#2278; 1:1000) and HA-Tag (C29F4; cat. #S724S; 1:1000) monoclonal antibodies (mAbs) were purchased from Cell Signaling Technology (Frankfurt, Germany). The γ-tubulin antibody (cat. #T5326; 1:5000) mAb was obtained from Sigma Aldrich (Munich, Germany). Strep-HRP (cat.#2-1509-001; 1:10000) mAb was obrained from IBA (Goettingen, Germany).Peroxidase-conjugated secondary mAbs (cat. #31432 and #31462; 1:2500) were obtained from Pierce (Thermo Scientific, St. Leon-Rot, Germany). Alexa Flour 488 conjugated Fab goat anti-rabbit IgG (cat. #A11070; 1:500) and mCherry antibody (PA5-34974; 1:1000) was received from Thermo Fisher Scientific (Waltham, USA).

Construction of SyCyRs and synthetic fluorescent ligands

SyCyR pcDNA3.1 expression plasmids were generated by fusion of coding sequence for the IL-11R signal peptide (Q14626, aa 1-22), a myc-tag (EQKLISEEDL; SyCyRs containing GFP_{VHH}) or a FLAG-tag (DYKDDDDK) and HA-tag (YPYDVPDYA; SyCyRs containing $mCherry_{VHH}$) followed by a nanobody (GFP_{VHH} or $mCherry_{VHH}$), some residues of the extracellular domain (ECD), the complete transmembrane (TMD) and complete intracellular domain (ICD) of the respective cytokine receptor. For the TNFR1-SyCyR and the TNFR2-SyCyR the coding cDNAs consist of 9 aa of the ECD and the complete TMD and ICD. The cDNA for the Fas-SyCyR consists of 10 aa of the ECD and the complete TMD and ICD of the receptor. The cDNAs for the TrailR1- and TrailR2-SyCyR consist of 10 aa of the ECD and the complete TMD and ICD. The gp130-SyCyR is made up of 13 aa from the ECD and the complete TMD and ICD. Mutation of the Fas death domain was generated by side directed mutagenesis using Phusion® high fidelity DNA polymerase (Thermo Fisher Scientific, Waltham, USA) followed by DpnI digestion of the methylated template DNA. All SyCyRs were inserted into pMOWS-hygro (Suthaus et al., 2011) ($mCherry_{VHH}$) or pMOWS-puro (Ketteler et al., 2003) (GFP_{VHH}) vectors for stable transfection of Ba/F3/gp130 cells. All generated cDNAs were verified by sequencing.

Generation of synthetic ligands

Synthetic ligands (sequences published in [Mossner et al., 2020b] and shown in supplemental information) were stably expressed in CHO-K1 cells using neomycin resistance and single clone selection with 1.125 mg/ml G-418 (Genaxxon, Ulm, Germany). Transfected cells were cultivated with G-418 for two weeks

and single clone selection was carried out with 0.5 cells/well. Single colonies were screened for protein expression. One clone was selected for protein expression in roller bottles (IBS Integra Biosciences, Zizers, Switzerland) with 10% low IgG fetal calf serum (GIBCO®, Life Technologies, Darmstadt, Germany) DMEM for two months. The supernatants were collected every 3-4 d and 1 L of supernatant was used for purification of Fc-tagged proteins using ProteinA MabSelect^{TM} HiTrap^{TM} columns (GE Healthcare, Chalfront St Giles, UK). Elution was carried out by pH shift using citrate buffer of pH 5.5 and 3.2. Buffer exchange to PBS was achieved using NAP^{TM}-25 columns (GE Healthcare, Chalfront St Giles, UK). GFP-mCherry fusion protein with Twin-Strep-tag was purified using StrepTrap^{TM} HP column (GE Healthcare, Chalfront St Giles, UK). Elution was carried out by competitive displacement with 2.5 mM Desthiobiotin. Buffer exchange to PBS was achieved using NAPTM-25 columns (GE Healthcare, Chalfront St Giles, UK).

Transfection and selection of cells

Ba/F3/gp130 cells were transduced retrovirally using pMOWS plasmids coding for SyCyRs. Phoenix-Eco cells were used as packaging cell line. pMOWs expression plasmids (5 μg) were transiently transfected in 6 x 10^5 Phoenix-Eco cells using Turbofect transfection reagent (Thermo Fisher Scientific, Waltham, USA). 250 μl of the obtained retroviral supernatants were mixed with 1 x 10^5 Ba/F3/gp130 cells and centrifuged for 2 h at 1800 rpm and RT with the addition of 8 μg/ml polybrene (Sigma Aldrich, Munich, Germany). Cells were selected with 1.5 μg/ml puromycin and/or 1 mg/ml hygromycin B for at least 2 weeks (Floss et al., 2013). After transduction cells were grown as described above and supplemented permanently with puromycin (1.5 μg/ml) and/or hygromycin B (1 mg/ml) (Carl Roth, Karlsruhe, Germany).

Cell viability assay

Ba/F3/gp130 cell lines were washed 3 times with PBS to remove cytokines from the medium. 5 x 10^4 cells were suspended in DMEM containing 10% FCS, 60 mg/l penicillin, and 100 mg/ml streptomycin. Cells were cultured for 3 d in a volume of 100 μl with or without cytokine/synthetic ligands. The CellTiter Blue Viability Assay (Promega, Karlsruhe, Germany) was used to determine the approximate number of viable cells by measuring the fluorescence (excitation 560 nm, emission 590 nm) using the Infinite M200 Pro plate reader (Tecan, Crailsheim, Germany). After adding 20 μl per well of CellTiter Blue reagent (point 0) fluorescence was measured approximately every 20 min for up to 2 h. For each condition of an experiment 3-4 wells were measured. All values were normalized by subtracting time point 0 values from the final measurement.

AnnexinV/7-AAD staining

Ba/F3/gp130 cell lines were washed 3 times with PBS. For the 24 h analysis, 2.5 x 10^5 cells and for the analysis after 48 h, 1.25 x 10^5 cells were used per well and incubated with the indicated cytokines. For the condition ethanol + Hyper-IL-6 or GFP-Fc cells were only incubated with Hyper-IL-6 or GFP-Fc. Ethanol was added to the washing steps right before the measurement. After the indicated time points, cells were washed twice with ice-cold PBS and if indicated also with 70% ethanol. Cells were resuspended in 300 μL Annexin V binding buffer (BD Bioscience, Franklin Lakes, USA) and 0.5 μL Annexin V (ImmunoTools, Oldenburg, Germany) were added. Cells were vortexed and incubated at room temperature for 15 min in the dark. Then 1 μL 7-AAD (R&D Systems, Minneapolis, USA) was added and 400 μL of AnnexinV binding buffer. Analysis was carried out by flow cytometry (BD FACSCanto II flow cytometer, BD Biosciences, San Jose, USA). Data was evaluated using FlowJo_V10 (FlowJo LLC, Ashland, USA).

Stimulation assay

Ba/F3/gp130 cells were washed 4 times with PBS to remove cytokines and starved in serum-free DMEM for 4 h. For TNFR stimulation 2.5 μM MG132 inhibitor (Sigma-Aldrich, St. Louis, USA) was added 30 min prior to stimulation. Cells incubated with IKK-2 inhibitor (Merck, Darmstadt, Germany) were pre-incubated with 18 μM IKK-2 30 min prior to stimulation. Cells were stimulated for 1 h with 100 ng/ml (or 0.1 –1000 ng/ml as indicated) purified protein, harvested, frozen in liquid nitrogen and then lysed. Stimulation of Fas-SyCyRs was carried out without serum starvation. Cells were directly stimulated in normal growth medium for 6 h with indicated cytokines. For stimulation of Fas-SyCyR cells with Caspase 3 inhibitor QVD, cells were again directly stimulated in normal growth medium for 2, 4 or 6 h. 10 μM QVD were added at the same time as the synthetic ligand. Cells were lysed for 1 h with lysis buffer containing 10 mM Tris-HCl, pH 7.8, 150 mM NaCl, 0.5 mM EDTA, 0.5% NP-40, 1 mM sodium vanadate, 10 mM $MgCl_2$ and a complete, EDTA-free protease inhibitor cocktail tablet (Roche Diagnostics, Mannheim, Germany). Protein concentration was determined by BCA Protein Assay (Thermo Fisher Scientific, Waltham, USA) as described by the

manufacturer. Protein expression and activation was analyzed as indicated by immunoblotting of 50 μg of each analysis.

Western blotting

50 μg of protein were loaded per lane, separated by SDS-PAGE under reducing conditions and transferred to a polyvinylidene fluoride (PVDF) membrane (Carl Roth, Karlsruhe, Germany). Blotting of membranes was performed with 5% fat-free dried skimmed milk (Carl Roth, Karlsruhe, Germany) in TBS-T (10 mM Tris-HCl pH 7.6, 150 mM NaCl, 0.5% Tween-20) for 4 h. Primary antibodies were diluted in 5% fat-free milk in TBS-T (STAT3, Caspase-3, γ-Tubulin, Strep-HRP) or 5% bovine serum albumin in TBS-T (pSTAT3, pIκB, IκB, GFP, mCherry) and incubated at 4°C overnight. Membranes were washed with TBS-T and then incubated with the secondary peroxidase-conjugated antibodies in 5% fat-free dried skim milk in TBS-T for at least 1 h. Membranes incubated with Strep-HRP were analyzed without secondary antibody. Signal detection was achieved using the ECL Prime Western Blotting Detection Reagent (GE Healthcare, Freiburg, Germany) and the Chemo Cam Imager (INTAS Science Imaging Instruments, Göttingen, Germany).

Coomassie staining

5 μg of protein were loaded per lane and separated by SDS-PAGE. The gel was stained with Coomassie staining solution (80% ethanol, 20% acetic acid, 4% Coomassie brilliant blue R250) for 20 min and washed twice with H_2O. The gel was then destained overnight in destaining solution (20% ethanol, 10% acetic acid) and scanned for analysis.

Cell surface detection of synthetic cytokine receptors

SyCyR expression of stably transfected Ba/F3/gp130 cells was detected by specific antibodies. Cells were washed in FACS buffer (PBS, 1% bovine serum albumin) and then resuspended in 50 μl FACS buffer containing indicated specific primary antibody (myc 1:100, HA 1:1000). After incubation of at least 1 h at room temperature, cells were washed and then resuspended in 50 μl FACS buffer containing secondary antibody Alexa Fluor 488 conjugated Fab goat anti-rabbit IgG (cat. # A11070; 1:500) and incubated for 1 h at room temperature. Cells were washed and resuspended in 500 μl FACS buffer and analyzed by flow cytometry (BD FACSCanto II flow cytometer, BD Biosciences, San Jose, USA). Data was evaluated using FlowJo_V10 (FlowJo LLC, Ashland, USA).

Quantitative RT-PCR

Cells were washed 4 times with PBS and then starved in serum-free DMEM for 4 h. They were stimulated with 100 ng/ml for 60 min as indicated, harvested and frozen in liquid nitrogen. RNA isolation was carried out using RNeasy Kit (Qiagen, Hilden, Germany). RNA concentration was determined by NanoDrop 2000c spectrophotometer (Thermo Scientific, Waltham, USA) and adjusted to 50 ng/μl for all samples. The expression of specific genes was determined by usage of iTaq^{TM} Universal SYBR Green One-Step Kit (Bio-Rad, Hercules, USA) as described previously (Fazel Modares et al., 2019). The expression level of FasL, Traf1, IL-6, Tnfα was normalized to the housekeeping gene glyceraldehyde 3-phosphate dehydrogenase (Gapdh) for relative quantification and calculated using the Δ(Ct1) method.

$$ratio = \frac{\left(\left(efficiency_{target} \times 0.01\right) + 1\right)^{ct_{target}}}{\left(\left(efficiency_{reference} \times 0.01\right) + 1\right)^{ct_{reference}}}$$

The expression level of target genes was determined by AB17500 Real-Time PCR System (Thermo Scientific, Waltham, USA). The following primer pairs were used in this study: GAPDH: fw 5′: GAAGGGCTCATG ACCACAGT, rev 5′: CATTGTCATACCAGGAAATGAGCT; FasL: fw 5′: GCGGGTTCGTGAAACTGATAA, rev 5′: GCAAAATGGGCCTCCTTGATA; Traf1: fw 5′: AGGGTGGTGGAATTACAGCAA, rev 5′: GCAGTGT AGAAAGCTGGAGAG; IL-6: fw 5′: CAAAGCCAGAGTCCTTCAGA, rev 5′: GATGGTCTTGGTCCTTAGCC; TNFα: fw 5′: CTGAACTTCGGGGTGATCGG, rev 5′: GGCTTGTCACTCGAATTTTGAGA.

QUANTIFICATION AND STATISTICAL ANALYSIS

Data are shown as mean ±SD. Multiple comparisons were determined with GraphPad Prism 6 (GraphPad Software, San Diego, CA, USA) using one-way ANOVA column analyses. Statistical significance was set to $p < 0.05$ (***$p < 0.001$, **$p < 0.01$, *$p < 0.05$).